JOC The Journal of Organic Chemistry

Article

pubs.acs.org/joc

3,5-Diarylimidazo[1,2-*a*]pyridines as Color-Tunable Fluorophores

Ju Young Lee,[†,∥] Jae Yul Shim,[†,∥] Hong Ki Kim,[‡,§] Donguk Ko,[†] Mu-Hyun Baik,*[,‡,§] and Eun Jeong Yoo*[,†]

[†]Department of Chemistry, Kangwon National University, 1 Kangwondaehak-gil, Chuncheon 24341, South Korea

[‡]Center for Catalytic Hydrocarbon Functionalizations, Institute for Basic Science (IBS), Daejeon 34141, South Korea

[§]Department of Chemistry, Korea Advanced Institute of Science and Technology (KAIST), Daejeon 34141, South Korea

Supporting Information

ABSTRACT: A new protocol for the synthesis of color-tunable fluorescent 3,5-diarylimidazo[1,2-*a*]pyridines has been achieved via palladium-catalyzed C−H amination of pyridinium zwitterions. Based on experimental results and computational analysis, we extracted a high correlation of photophysical properties with the theoretical concept and predicted emission wavelengths of 3,5-diarylimidazo[1,2-*a*]pyridines. The emission wavelengths of imidazo[1,2-*a*]pyridines increase as a function of the electron-withdrawing nature of the substituent on the C5-aryl group of imidazo[1,2-*a*]pyridine as a result of inductive effects on the LUMO levels. Varying the substituent on the C3-aryl group imidazo[1,2-*a*]pyridine changes the HOMO levels. Combining these two sites, the HOMO and LUMO levels can be tuned fairly decoupled from each other. This conceptual trend is demonstrated across a series where the C3 and C5 positions were functionalized independently and then utilizes a combination strategy where both sites are used to prepare fluorophores with a large window of emission wavelengths. In view of the biological properties of imidazo[1,2-*a*]pyridines, the developed method provides an efficient approach for understanding and preparing strongly fluorescent bioprobes.

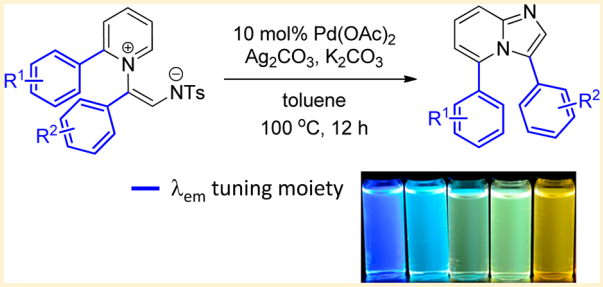

INTRODUCTION

Fluorophores are an important class of compounds with diverse applications, for example, in the fields of biomedical and photoelectric materials.[1] N-Heterocycles often form the π-conjugated core structure, and N-fused heterocycles are particularly prominent among tunable fluorophores,[2] with aryl functionalities being beneficial for the fluorescence intensity but also enabling the tuning of the emission wavelength (λ_{em}) (Scheme 1). For instance, Park and co-workers developed a color-tunable fluorophore named Seoul-Fluor, which shows full color emissions modulated by the aryl moiety at the C1 position and R^2 group.[2a,b] The 1,3a,6a-triazapentalene derivatives reported by Namba, Tanino, et al. exhibit various fluorescence colors because of the inductive effect of the 2-aryl substituents.[2c,d] Moreover, the group of Lan, You, et al. prepared libraries of color-tunable fluorescence compounds by introducing various aromatic groups in C3-Indo-Fluor.[2e] Despite the understanding of the relationship between structure and photophysical property, the design of color-tunable fluorophores giving access to a broad palette of colors remains a challenge.

Imidazo[1,2-*a*]pyridines are involved in many biological processes relevant to medicinal applications and are one of the most widely used N-fused heterocycles.[3] Imidazo[1,2-*a*]-pyridines are also crucial in the optoelectronics and organometallic chemistry, where they serve as excited-state intramolecular proton transfer (ESIPT) fluorophores,[4] for example.

Scheme 1. Color-Tunable Fluorophores Based on N-Fused Heterocycles

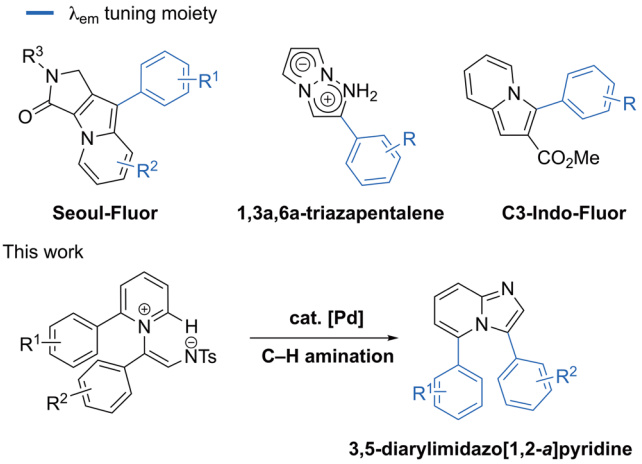

Whereas the preparation of 2- or 3-arylimidazo[1,2-*a*]pyridines has received considerable attention,[5] modifications of the pyridine skeleton of imidazo[1,2-*a*]pyridines have been less explored.[6] In particular, straightforward methods to access diarylimidazo[1,2-*a*]pyridines are rare. In most cases, the

Received: February 14, 2017
Published: March 28, 2017

DOI: 10.1021/acs.joc.7b00358
J. Org. Chem. 2017, 82, 4352−4361

synthetic routes to π-extended imidazo[1,2-*a*]pyridines are tedious because they require the use of halogen-substituted imidazo[1,2-*a*]pyridines as reactants for the cross-coupling reactions. Recently, we developed an isolable, bench-stable pyridinium zwitterion that can serve as a 1,5-dipole in the formation of N-heterocycles.[7a] The thermal [5 + 2] cycloaddition and catalytic [5 + 3] cycloaddition of pyridinium zwitterions were reported for the synthesis of seven-membered and eight-membered N-heterocycles, respectively.[7] Encouraged by these achievements, we envisioned that π-conjugated imidazo[1,2-*a*]pyridines could be efficiently synthesized by intramolecular cyclization of a pyridinium zwitterion in a single operation (Scheme 1). In addition, we envisioned that this platform may be an ideal candidate for a fluorophore that can be tuned over a wide range of colors since the extended π-conjugation across the bicycle can be exploited to construct a highly decorated class of fluorophores.[4a,8]

RESULTS AND DISCUSSION

Whereas there is little doubt that the electronic excitation in this system is a π−π* transition, constituting an intramolecular charge transfer (ICT), it is not at all clear which position of the imidazo[1,2-*a*]pyridine skeleton may be the most effective site for functionalization. Roughly, we may approximate the absorption and fluorescence energies as the HOMO−LUMO gap. Figure 1 illustrates the shapes of these frontier orbitals.

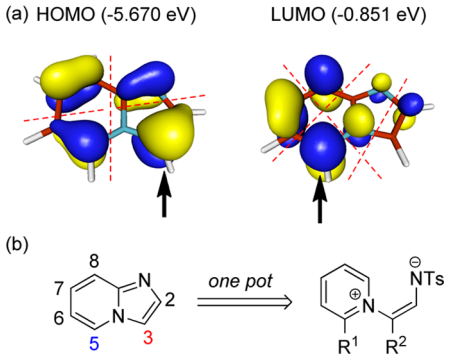

Figure 1. (a) Isosurface plots (isodensity value = 0.05 a.u.) of HOMO and LUMO of the core imidazo[1,2-*a*]pyridine skeleton. (b) Selected tunable sites of imidazo[1,2-*a*]pyridine and synthetic strategy.

The HOMO is simply a π-orbital with two nodes, whereas the LUMO is a π*-orbital with three nodes, as indicated in Figure 1a. Simply inspecting the shapes of these orbitals reveals an intuitive strategy for tuning their energies: The HOMO shows a significant orbital contribution at the C3 position, and therefore, any substituent connected to C3 imposing a π-inductive effect will directly modulate the HOMO energy. Electron-donating groups will raise the HOMO energy, whereas electron-withdrawing groups will lower it. Interestingly, there is no contribution of C3 to the LUMO, as illustrated by Figure 1a.

Consequently, electronic modulations at the C3 position will mostly impact the HOMO but have only a minor impact on the energy of the LUMO. Similarly, the C5 position is the most promising site of functionalization to control the LUMO energy, as the π-orbital at C5 is the major contributor to the LUMO. Unfortunately, the π-orbital of the C5-atom also plays a notable role in shaping the HOMO. Thus, functionalizations at this position will impact both the LUMO and HOMO. Since the size differences are significant, it is reasonable to assume that the LUMO will be more sensitive to C5-functionalizations than HOMO. In concert, these two positions should allow for substantial changes of the HOMO−LUMO gap, thus enabling the color of the fluorophore to be changed with relative ease over a wide range. As is always the case with frontier orbital based strategies, there is some uncertainty about how structural changes that are inevitably introduced by the functionalization will impact the frontier orbitals. To assess these effects quantitatively, we have carried out density functional theory (DFT) calculations on all derivatives and calculated the photophysical properties specifically using time-dependent DFT methods. The combination of frontier orbital based qualitative assessment and numerical evaluation of the emission characteristics provides a solid conceptual foundation for understanding the experimental results.

Synthesis. Based on the electrocyclization of azomethine ylides and azomethine imines, we expected 3,5-diarylimidazo-[1,2-*a*]pyridines (**2a**) to be formed by 1,5-electrocyclization[9] of pyridinium zwitterions (**1a**); thus, reaction temperature and additives, factors known to positively influence the electrocyclization process, were screened. However, the desired product (**2a**) was not observed in these studies because of the thermal stability of the pyridinium zwitterion. This observation prompted us to turn our attention to the cyclization of pyridinium zwitterions via catalytic C−H amination (Scheme 2).[10] In this approach, Pd(II) first binds

Scheme 2. Synthetic Approaches to 3,5-Diarylimidazo[1,2-*a*]pyridine

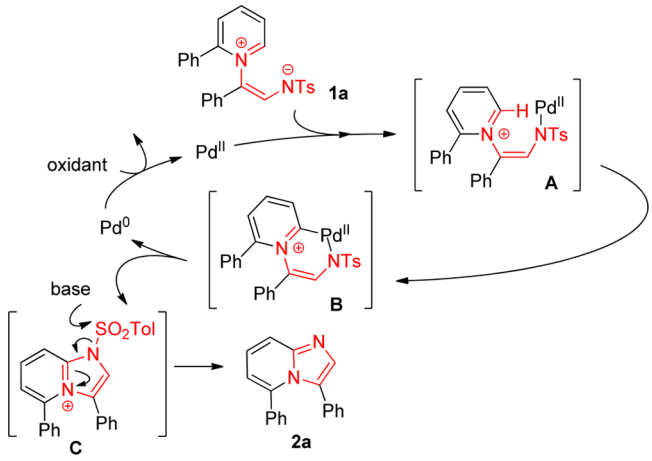

to the pyridinium zwitterion (**1a**) affording adduct **A**, which is readily converted to intermediate **B** via C−H activation. Next, 3,5-diarylimidazo[1,2-*a*]pyridine (**2a**) is obtained by reductive elimination and subsequent desulfonylation,[11] which rearomatizes to drive the overall reaction forward. Finally, in the presence of an excess amount of oxidant, Pd(0) is reoxidized to Pd(II), available for another catalytic cycle.

With this mechanistic hypothesis in mind, we sought to subject the pyridinium zwitterion (**1a**) to various reaction conditions to produce the corresponding 3,5-diphenylimidazo-[1,2-*a*]pyridine (**2a**) (Table 1). As expected, the product **2a** was not obtained in the absence of one of the three agents, i.e. palladium catalyst, oxidant, and base (entries 1 and 2). Whereas oxygen gas and hypervalent iodine oxidant were unable to increase the catalytic turnover, copper- and silver-based oxidants were found to be suitable for this transformation

DOI: 10.1021/acs.joc.7b00358
J. Org. Chem. 2017, 82, 4352−4361

Table 1. Optimization of Reaction Conditions[a]

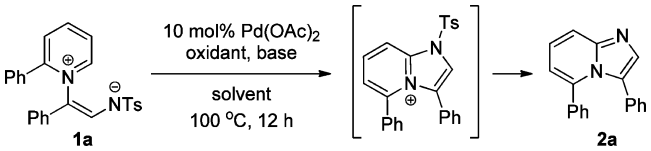

entry	oxidant	base	solvent	yield[b] (%)
1			toluene	<1
2	Ag_2CO_3	K_2CO_3	toluene	<1[c]
3	O_2	K_2CO_3	toluene	<1
4	$PhI(OAc)_2$	K_2CO_3	toluene	<5
5	CuOAc	K_2CO_3	toluene	43
6	AgOAc	K_2CO_3	toluene	32
7	Ag_2CO_3	K_2CO_3	toluene	85
8	Ag_2CO_3	K_2CO_3	benzene	63
9	Ag_2CO_3	K_2CO_3	1,2-DCE	<1
10	Ag_2CO_3	K_2CO_3	THF	5
11	Ag_2CO_3	Li_2CO_3	toluene	30
12	Ag_2CO_3	NaOAc	toluene	52
13	Ag_2CO_3	Et_3N	toluene	57

[a]Reaction conditions: **1a** (0.2 mmol), $Pd(OAc)_2$ (10.0 mol %), oxidant (1.5 equiv), base (2.0 equiv), and solvent (1.0 mL) at 100 °C for 12 h. [b]^1H NMR yields using CH_2Br_2 as an internal standard. [c]Reaction was carried out without $Pd(OAc)_2$.

(entries 3–6). Gratifyingly, pyridinium zwitterion **1a** afforded the desired product **2a** in 85% yield using $Pd(OAc)_2$ (10 mol %), Ag_2CO_3 (1.5 equiv), and K_2CO_3 (2.0 equiv) as the catalyst, oxidant, and the base, respectively, in toluene at 100 °C (entry 7). After a number of solvents were surveyed, the solubility of pyridinium zwitterion was found to not improve the cyclization (entries 7–10). By changing the base from K_2CO_3 to other inorganic and organic bases, such as Li_2CO_3, NaOAc, and Et_3N, cyclization was less effective (entries 11–13).

Under the optimized conditions, a range of pyridinium zwitterions underwent smooth cyclization to afford the corresponding 3,5-diarylimidazo[1,2-*a*]pyridines in good yields. First, the effect of the nature of the R^1 substituent on the pyridinium backbone of **1** was investigated (Table 2). Zwitterions with electron-donating groups, such as methoxy, *tert*-butyl, and methyl on the phenyl ring delivered the desired products in moderate to good yields regardless of the position of substituent (**2a–e**). The reaction conditions were also compatible with halide groups (**2f** and **2g**). However, the efficiency of this reaction was affected by electronic properties of the 2-arylpyridinium zwitterions, and thus, lower yields were obtained using zwitterions with electron-poor substituents (**2h** and **2i**). A naphthyl-containing substrate readily reacted, resulting in the formation of the desired product (**2j**) in 73% yield.

Next, we surveyed the substrate scope by varying the R^2 group on the pyridinium zwitterions (Table 3). Pleasingly, substrates containing both electron-rich and electron-deficient substituents cyclized smoothly, affording the desired products in moderate yields (**2k–q**). The tolerance of the bromo group (**2n**) is particularly useful because it allows subsequent palladium-catalyzed coupling reactions. Moreover, the cyclization of most of the *meta*-substituted pyridinium zwitterions proceeded in a facile manner, affording **2r–t** in good yield (84–70%).

Encouraged by these results, we attempted to synthesize 3,5-diarylimidazo[1,2-*a*]pyridines having a donor–acceptor system

Table 2. Synthesis of C5-Functionalized Imidazo[1,2-*a*]pyridines[a,b]

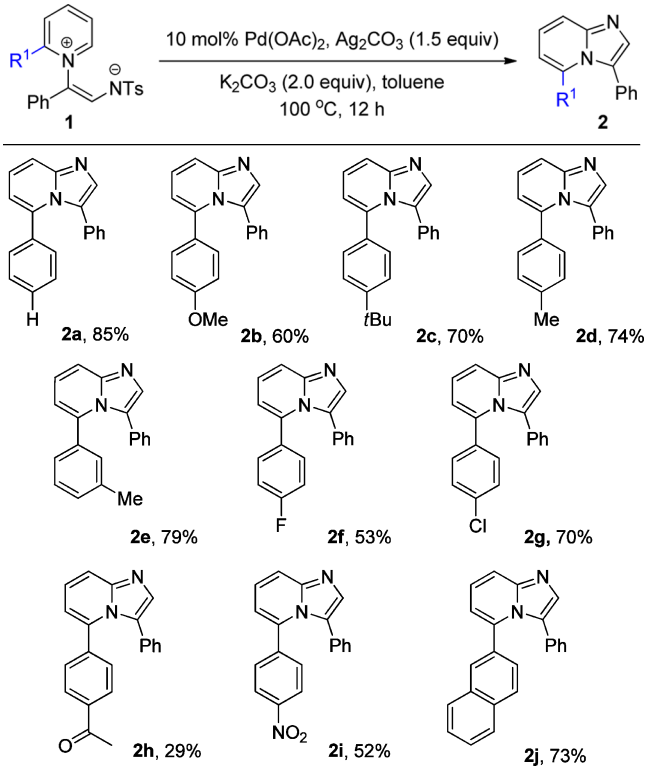

[a]Reaction conditions: **1** (0.2 mmol), $Pd(OAc)_2$ (10.0 mol %), Ag_2CO_3 (1.5 equiv), K_2CO_3 (2.0 equiv), and toluene (1.0 mL) at 100 °C for 12 h. [b]Isolated yields.

(Table 4, **2u–w**). To our delight, the optimized reaction conditions afforded the desired products albeit in slightly low yields. Satisfyingly, in addition to the 2-aryl group, the 3-alkyl substituent was readily introduced into the imidazo[1,2-*a*]pyridine skeleton (3,5,6-trisubstituted imidazo[1,2-*a*]-pyridine, **2x**). It is worth noting that this catalytic transformation could also be applied to the synthesis of other π-conjugated structures, namely imidazo[1,2-*a*]quinolines (Scheme 3).[12] Several quinolinium zwitterions (**3**) underwent cyclization without further optimization, affording the desired products (**4a–d**) in 37–48% yields.

Fluorophore Design Strategy. The library of fluorophores prepared in this study can be divided into three categories, where **2a** bearing phenyl groups at both the C3 and C5 positions serves as the reference fluorophore: (i) the first group consists of **2b–j**, where the phenyl functionality bound to C5 is systematically varied at the para-position, as enumerated in Table 2. (ii) The second series contains molecules where the phenyl at C3 was derivatized, as shown in Table 3. (iii) Finally, Table 4 shows four donor–acceptor fluorophores where both the C3 and C5 positions carry functionalized phenyl groups.

As explained above, the C5 position is expected to exert direct control over the LUMO, whereas the HOMO should be affected to a lesser degree, in **2b–j**. Functionalizations at the C3 position should not have any direct impact on the LUMO but influence the HOMO as in **2k–t**. Thus, we expect to see a more dramatic variance of HOMO–LUMO gaps in the first series, which should translate into a wider range of colors. Figure 2 compares the HOMO and LUMO energies as a

DOI: 10.1021/acs.joc.7b00358
J. Org. Chem. 2017, 82, 4352–4361

Table 3. Synthesis of C3-Functionalized Imidazo[1,2-*a*]pyridines[a,b]

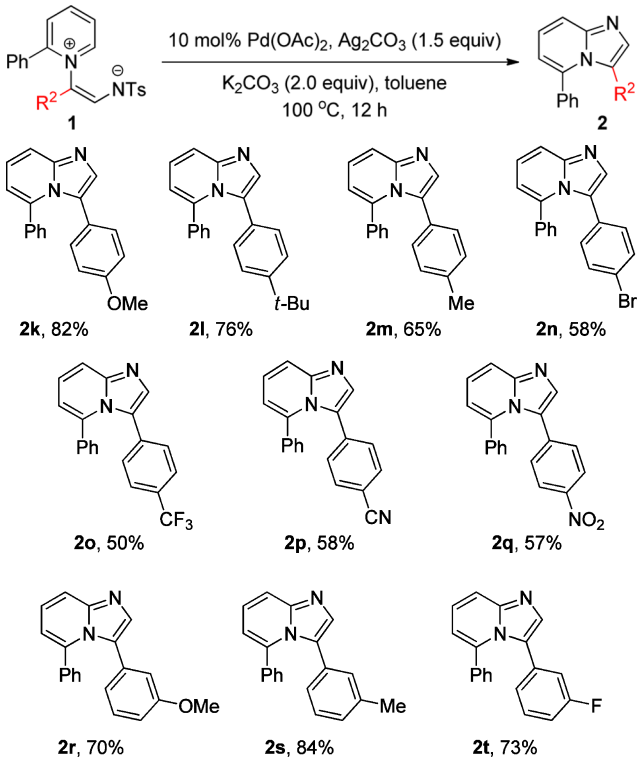

[a]Reaction conditions: **1** (0.2 mmol), $Pd(OAc)_2$ (10.0 mol %), Ag_2CO_3 (1.5 equiv), K_2CO_3 (2.0 equiv), and toluene (1.0 mL) at 100 °C for 12 h. [b]Isolated yields.

Table 4. 3,5-Disubstituted Imidazo[1,2-*a*]pyridine with Various Arenes[a]

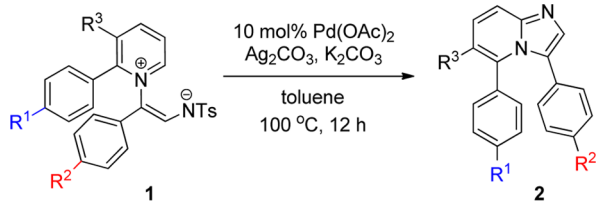

compd	R^1	R^2	R^3	yield[b] (%)
2u	OMe	CN	H	35
2v	COMe	OMe	H	42
2w	NO_2	OMe	H	32
2x	H	H	Me	65

[a]Reaction conditions: **1** (0.2 mmol), $Pd(OAc)_2$ (10.0 mol %), Ag_2CO_3 (1.5 equiv), K_2CO_3 (2.0 equiv), and toluene (1.0 mL) at 100 °C for 12 h. [b]Isolated yields.

function of the Hammett constant[13] (σ) of the functional groups R^1 and R^2. As expected, all frontier orbitals move to lower energies in general when the phenyl substituent becomes more electron withdrawing. Interestingly, the HOMO energies illustrated by filled squares in Figure 2 change in a consistent fashion across both the first and second series of fluorophores. In other words, it does not matter whether the C3 or C5 positions are used for attaching the functional group; they have a very similar impact on the HOMO energy. This finding is in good agreement with the shape of HOMO shown in Figure 1a,

Scheme 3. Synthesis of Imidazo[1,2-*a*]quinolines via C−H Amination

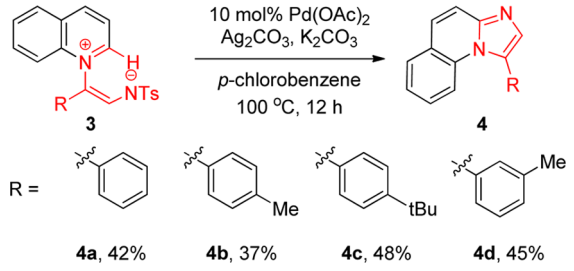

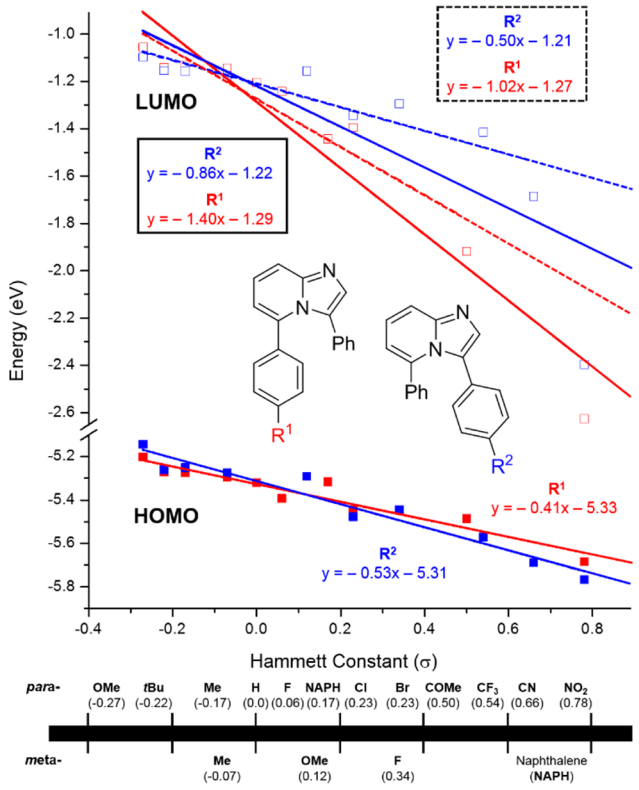

Figure 2. Calculated HOMO and LUMO energies for C5-functionalized imidazo[1,2-*a*]pyridines (**2a−j**; red color) and C3-functionalized imidazo[1,2-*a*]pyridines (**2k−t**; blue color), respectively.

which has almost equal contributions from both the C3 and C5 π-orbitals.

The changes in the LUMO energies are remarkably different. As shown in the empty squares in Figure 2, derivatizing the imidazopyridine skeleton at the C5-position gives access to a much wider LUMO energy range, shown as a solid red line in Figure 2. The trend line indicates a slope of −1.40, which is much steeper than −0.41 seen for the corresponding HOMO levels. In contrast, the slope of the trend line for the LUMO energies for the C3-functionalized analogues, shown as a solid blue line, is only −0.86. Analyzing the LUMO energies more closely, it is clear that the LUMO of the strongly electron-withdrawing nitro group distorts the overall trend notably, as both **2i** and **2q** have LUMO energies that are much lower than the other molecules. Thus, we obtained partial trend lines excluding **2i** and **2q** and show them as broken lines in Figure 2. The C5-functionalized series still shows a slope of −1.02, which is notably steeper than the HOMO trend line, but the C3-functionalized series displays a slope of only −0.50, which is

DOI: 10.1021/acs.joc.7b00358
J. Org. Chem. 2017, 82, 4352−4361

practically identical to that of −0.53 found for the HOMO levels. If the energy trends of the HOMO and LUMO energies are identical, the HOMO → LUMO transitions will be identical as well, and consequently, the variance in the color of the fluorophores will be minimal.

In summary, the analysis of the frontier orbitals indicates that functionalizing the imidazopyridine skeleton at the C5 position is a superior strategy for color tuning and gives direct control over the LUMO levels, which in principle should allow for a wider color range than C3 functionalizations. The principle highlighted in the trends shown in Figure 2 also suggests a promising new strategy: Since placing electron-withdrawing groups on C5 lower the LUMO energies, while placing electron-donating groups on the C3 position raises the HOMO levels and the LUMO energy tuning is disconnected from the C3 position, we should be able to engineer a very narrow HOMO−LUMO gap by placing an electron-withdrawing group on C5 and an electron-donating group on C3. The opposite functionalization scheme should afford a large HOMO−LUMO gap. To test this combination strategy, we prepared the donor−acceptor fluorophores **2u**−**x**, shown in Table 4. Because it was synthetically convenient, we have also used imidazo[1,2-*a*]quinolines to carry out the C−H amination using our methodology and obtained the fluorophores **4a**−**d**. As the expansion of the π-conjugation affects the LUMO that is centered at the C5 position, we can envision the ring fusion formally as a [4 + 2] cycloaddition of a butadiene onto the C5═C6 dienophile, which will push the LUMO energies higher. Thus, we expect the emissions to be blue-shifted.

Photophysical Properties. With the qualitative predictions discussed above in hand, the photophysical properties were examined and theoretical studies using time-dependent density functional theory[14] (TD-DFT) with Tamm−Dancoff approximation (TDA)[15] were carried out.[16] The TDA applied to the TD-DFT methods reduces the instability of TD-DFT calculations near state junctions.[17] The energy and surface plots of the HOMOs and LUMOs in each compound are given in the Supporting Information. The ground state (S_0) and the first excited singlet state (S_1) geometries have been optimized in both the gas- and solvent-phase since the solvent can be significantly influence the emission,[18] but we found that the gas-phase calculations gave slightly better agreement with experimental results and the difference is small (∼10 nm) and physically not meaningful. We show here the gas-phase calculation results. The experimentally determined photophysical properties are summarized in Table 5 and illustrated in Figure 3.

The TD-DFT-calculated emissions are enumerated in the Supporting Information and indicated in Figure 3. A handful fluorophores such as **2c**, **2e**, **2f**, or **2i** that either showed very weak photophysical activities or were otherwise uninteresting were not recorded. Based on the orbital analysis described above, we expected that the higher electron-withdrawing ability of R^1 substituent will result in bathochromic shifts in the emission wavelength (**2b**−**h**) as the HOMO−LUMO gap becomes smaller. As predicted, the R^1 substituent gives access to a notably wider emission range of 38 nm, spanning from 468−506 nm, while the R^2 substituent (**2k**−**p**) allows a tunable range of 27 nm from 457−484 nm, as illustrated in Figure 3. The theory−experiment correlation is reasonable, and we observed that the TD-DFT method generally underestimates the emission wavelengths systematically by ∼10 nm across the whole series. More importantly, the trends seen in the experiment indicate that C5 functionalization leads to a more monotonically consistent trend with increasing emission wavelengths as a function of increasing Hammett constant, whereas C3 functionalization gives a less well-defined scatter within a narrower range. The push−pull systems **2u** and **2v** that were designed to show very short and very long emission wavelengths consistent with a very large and very small HOMO−LUMO gap, respectively, exhibited the anticipated photophysical properties. The emission wavelength of **2v** was found to be 537 nm, which is by far the longest wavelength found in this series of fluorophores, whereas **2u** showed an

Table 5. Photophysical Properties of π-Extended Imidazo[1,2-*a*]pyridines[a]

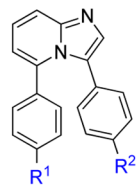

imidazo[1,2-*a*]pyridine (**2**)

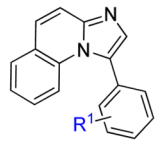

imidazo[1,2-*a*]quinoline (**4**)

compd	R^1	R^2	λ_{abs}[b] (nm)	λ_{em} (nm)	log ε	Stokes shift (nm)	Φ
2a	H	H	337	473	3.74	136	0.24
2b	OMe	H	332	468	3.79	136	0.21
2d	Me	H	341	470	3.78	129	0.28
2f	F	H	336	469	3.84	133	0.32
2g	Cl	H	338	478	3.67	140	0.42
2h	COMe	H	358	506	3.68	148	0.43
2k	H	OMe	341	484	3.57	143	0.26
2l	H	*t*-Bu	339	479	3.66	140	0.31
2p	H	CN	331	457	4.35	126	0.19
2u	OMe	CN	329	447	4.20	118	0.17
2v	COMe	OMe	366	537	3.91	171	0.10
4b	*p*-Me		324	424	3.93	100	0.42
4d	*m*-Me		325	425	3.96	100	0.55

[a]Photophysical properties in CH_2Cl_2 at 20.0 μM. [b]Only the longest absorption maxima are shown.

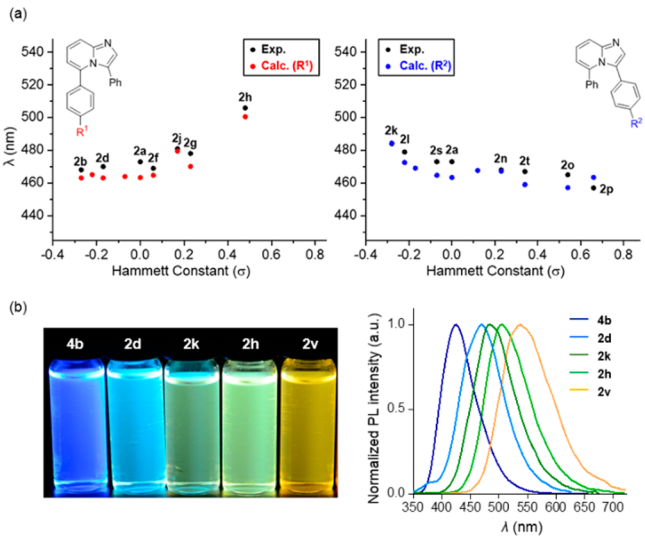

Figure 3. (a) Scatter plots of the emission wavelength of 3,5-diarylimidazo[1,2-*a*]pyridine with various substituents. (b) Fluorescence images of imidazo[1,2-*a*]pyridines in CH_2Cl_2 irradiated at 365 nm.

DOI: 10.1021/acs.joc.7b00358
J. Org. Chem. 2017, 82, 4352−4361

emission at 447 nm, the shortest emission wavelength seen in the series. The difference between these two extreme cases constitutes a remarkable 90 nm. The imidazo[1,2-*a*]quinolines **4b** and **4d** displayed hypsochromically shifted emission maxima at 424 and 425 nm and high quantum yields, which are in good agreement with the anticipated raising of the LUMO levels due to the quinoline moiety. Notably, these new fluorophores showed large Stokes shifts, which is an attractive property for the fluorogenic bioprobe.

CONCLUSION

In conclusion, the fluorescence of 3,5-diarylimidazo[1,2-*a*]-pyridine was found to originate from the $\pi-\pi^*$ transitions of the imidazo[1,2-*a*]pyridine skeleton, which is not surprising. A quantum chemical frontier orbital analysis emphasized that the C5 position of the core structure is an ideal site for installing a functional group handle for the fine-tuning of the photophysical activity, as it is eminently involved in determining the nature of the LUMO, while the C3 position is not at all involved in the LUMO. The HOMO, on the other hand, showed a significant orbital amplitude at the C3 position, therefore establishing that functionalization at this position will impact the HOMO levels, while functionalizations of the C5 positions will impact the LUMO levels in a fairly independent fashion. These two-point handles should in principle allow for the widening the window of accessible colors. To conveniently access these 3,5-diarylimidazo[1,2-*a*]pyridine fluorophores, we have utilized a palladium-catalyzed C−H amination reaction of pyridinium zwitterions that we have developed recently in our laboratory. The resulting π-extended imidazo[1,2-*a*]pyridine fluorophores exhibited continuously tunable emission wavelengths with high quantum yields, as anticipated. The power of this conceptual insight is emphasized by logically extending the conceptual basis to prepare push−pull substituent combinations, where we can understand and engineer an emission wavelength difference as large as 90 nm using the same set of substituents by simply exchanging their positions. The value and conceptual meaning of the C5-functionalizations have thus far been under-appreciated.

EXPERIMENTAL SECTION

General Methods. Unless otherwise stated, all commercial reagents including catalysts and solvents were used without additional purification. The pyridinium zwitterions and quinolinum zwitterions were prepared according to the reported procedure.[7a] Analytical thin-layer chromatography (TLC) was performed on Merck precoated silica gel 60 F254 plates. Visualization on TLC was achieved by use of UV light (254 nm). Flash column chromatography was undertaken on silica gel (Merck Kiesel gel 60 F254 230−400 mesh). ^{1}H NMR was recorded on Bruker DPX FT (300 and 400 MHz). Chemical shifts were quoted in parts per million (ppm) referenced to the appropriate solvent peak or 0.0 ppm for tetramethylsilane. The following abbreviations were used to describe peak splitting patterns when appropriate: br = broad, s = singlet, d = doublet, t = triplet, q = quartet, m = multiplet. Coupling constants, *J*, are reported in hertz (Hz). ^{13}C NMR was recorded on a Bruker FT AM 400 (100 MHz) and was fully decoupled by broad-band proton decoupling. Chemical shifts were reported in ppm referenced to the center line of a triplet at 77.0 ppm of chloroform-*d*. Infrared spectra were recorded on a JASCO FT/IR-460 plus FT-IR spectrometer. Frequencies are given in reciprocal centimeters (cm^{-1}), and only selected absorbance is reported. High-resolution mass spectra were obtained from the Korea Basic Science Institute (Daegu) by electron impact (EI) and fast atom bombardment (FAB) using a magnetic sector−electric sector double-focusing mass analyzer. Absorption spectra were obtained on a Varian Cary 100 conc spectrometer. Fluorescence spectra and absolute quantum yields were collected on a Scinco FluoroMate FS-2 fluorescence spectrometer with a calibrated integrating sphere system.

Computational Details. All calculations were performed using density functional theory[19] (DFT) as implemented in the Jaguar 9.1[20] suite of ab initio quantum chemistry programs. The geometry optimizations were performed with the B3LYP[21] hybrid exchange and correlation functional. The 6-31G** basis set was used for all atoms,[22] which were represented by the Los Alamos LACVP basis set including relativistic effective core potential.[23] The HOMO and LUMO energies of the optimized structures were reevaluated by single-point calculations using Dunning's correlation consistent triple-ζ basis set cc-pVTZ(-f) that includes a double set of polarization functions.[24] Calculations for solvent effect were conducted by a self-consistent reaction field (SCRF) approach,[25] in which dichloromethane (CH_2Cl_2) was regarded as the continuum with the dielectric constant ε = 9.08. Furthermore, time-dependent DFT[14](TD-DFT) calculations with a Tamm−Dancoff approximation[15] (TDA) are used to optimize the structure of ground states and first excited states of the nature for the emission parameter. The isosurface plots of MOs were obtained by using the Molden software[26] and Cortorna3D.[27]

General Procedure for the Optimization Studies (Table 1). To a 2 mL screw capped vial with a triangular-shaped stir bar were added pyridinium 1,5-zwitterion (**1a**, 0.2 mmol), $Pd(OAc)_2$ (10.0 mol %), oxidant (1.5 equiv), base (2.0 equiv), and solvent (1.0 mL). The reaction mixture was stirred at 100 °C for 12 h, filtered through a pad of Celite, and then washed with ethyl acetate (10 mL × 3). Organic solvents were removed under reduced pressure. The NMR yield of desired product **2a** was determined by integration using an internal standard (CH_2Br_2).

Procedure for the Synthesis of Various Imidazo[1,2-*a*]-pyridines (Tables 2−4). To a 2 mL screw capped vial with a triangular-shaped stir bar were added pyridinium 1,5-zwitterion (**1**, 0.2 mmol), $Pd(OAc)_2$ (10.0 mol %), Ag_2CO_3 (1.5 equiv), K_2CO_3 (2.0 equiv), and toluene (1.0 mL). The reaction mixture was stirred at 100 °C for 12 h, filtered through a pad of Celite, and then washed with ethyl acetate (10 mL × 3). Organic solvents were removed under reduced pressure. The organic residue was purified by chromatography on silica gel (EtOAc/hexane = 1:1) to give the desired product **2**.

Procedure for the Synthesis of Imidazo[1,2-*a*]quinolines (Scheme 3). To 2 mL screw-capped vial with a triangular-shaped stir bar were added pyridinium 1,5-zwitterion (**3**, 0.2 mmol), $Pd(OAc)_2$ (10.0 mol %), Ag_2CO_3 (1.5 equiv), K_2CO_3 (2.0 equiv), and *p*-chlorobenzene (1.0 mL). The reaction mixture was stirred at 100 °C for 12 h, filtered through a pad of Celite, and then washed with ethyl acetate (10 mL × 3). Organic solvents were removed under reduced pressure. The organic residue was purified by chromatography on silica gel (EtOAc/hexane = 1:1) to give the desired product **4**.

*(Z)-(2-(2-(4-Nitrophenyl)pyridin-1-ium-1-yl)-2-phenylvinyl)(tosyl)-amide (**1i**):* purple solid (78.4 mg, 83%); mp 175.8−177.0 °C; ^{1}H NMR (400 MHz, $CDCl_3$) δ 8.57 (dd, *J* = 6.2, 1.0 Hz, 1H), 8.50 (td, *J* = 7.9, 1.5 Hz, 1H), 8.07−8.04 (m, 1H), 7.89 (dd, *J* = 8.0, 1.0 Hz, 1H), 7.80 (s, 1H), 7,76−7,72 (m, 2H), 7.61−7.59 (m, 2H), 7.40−7.37 (m, 2H), 7.18 (d, *J* = 7.9 Hz, 2H), 7.13−7.09 (m, 2H), 7.00−6.96 (m, 1H), 6.61−6.59 (m, 2H), 2.43(s, 3H); ^{13}C NMR (100 MHz, $CDCl_3$) δ 156.2, 150.5, 148.8, 144.9, 143.0, 140.7, 140.3, 137.6, 136.3, 129.9, 129.2, 129.1, 129.0, 127.9, 125.8, 124.9, 123.1, 120.5, 116.1, 21.3; IR (liquid) ν 3056.6, 2989.1, 2861.8, 1589.1, 1519.6, 1348.0, 1238.4, 1130.1, 1080.9 cm^{-1}; HRMS (FAB) *m*/*z* calcd for $C_{26}H_{21}N_3O_4S$ [M + H] 472.1331, found 472.1334.

*(Z)-(2-(4-Cyanophenyl)-2-(2-phenylpyridin-1-ium-1-yl)vinyl)-(tosyl)amide (**1p**):* red solid (76.9 mg, 85%); mp 135.1−137.7 °C; ^{1}H NMR (400 MHz, $CDCl_3$) δ 8.49 (td, *J* = 7.8, 1.4 Hz, 1H), 8.44−8.43 (m, 1H), 8.05 (s, 1H), 8.01−7.97 (m, 1H), 7.91−7.89 (m, 1H), 7.68 (d, *J* = 8.2 Hz, 2H), 7.32−7.27 (m, 1H), 7.24−7.18 (m, 6H), 7.08−7.04 (m, 2H), 6.50 (d, *J* = 8.6 Hz, 2H), 2.39 (s, 3H); ^{13}C NMR (100 MHz, $CDCl_3$) δ 158.2, 150.4, 145.2, 143.9, 142.3, 140.7, 140.7, 132.3, 131.3, 131.2, 130.2, 129.1, 128.3, 128.0, 127.1, 125.9, 119.5, 119.3, 115.5, 105.9, 21.3; IR (liquid) ν 3059.5, 2985.3, 2823.3, 2217.7,

DOI: 10.1021/acs.joc.7b00358
J. Org. Chem. 2017, 82, 4352−4361

1569.8, 1479.1, 1316.2, 1254.5, 1133.0, 1081.9 cm^{-1}; HRMS (FAB) m/z calcd for $C_{27}H_{21}N_3O_2S$ [M + H] 452.1433, found 452.1430.

*(Z)-(2-(4-Nitrophenyl)-2-(2-phenylpyridin-1-ium-1-yl)vinyl)(tosyl)-amide (**1q**):* red solid (73.9 mg, 78%); mp 156.5−157.4 °C; ^{1}H NMR (400 MHz, DMSO d_6) δ 8.90 (d, J = 5.6 Hz, 1H), 8.81−8.77 (m, 1H), 8.28−8.23 (m, 2H), 8.15 (s, 1H), 7.88 (d, J = 9.1 Hz, 2H), 7.55 (d, J = 8.1 Hz, 2H), 7.36−7.29 (m, 3H), 7.21 (d, J = 7.3 Hz, 2H), 7.09−7.05 (m, 2H), 6.82 (d, J = 9.0 Hz, 2H), 2.38 (s, 3H); ^{13}C NMR (100 MHz, DMSO d_6) δ 156.8, 150.4, 146.8, 145.2, 143.3, 142.4, 141.8, 140.4, 131.7, 130.7, 130.7, 129.1, 128.2, 127.9, 127.8, 125.5, 124.4, 118.6, 115.1, 20.9; IR (solid) ν 3061.4, 2984.3, 2928.3, 1558.2, 1495.5, 1322.9, 1251.6, 1134.9, 1108.9, 1078.9, cm^{-1}; HRMS (FAB) m/z calcd for $C_{26}H_{21}N_3O_4S$ [M + H] 472.1331, found 472.1332.

*(Z)-(2-(4-Cyanophenyl)-2-(2-(4-methoxyphenyl)pyridin-1-ium-1-yl)vinyl)(tosyl)amide (**1u**):* red solid (77.3 mg, 80%); mp 165.8−168.7 °C; ^{1}H NMR (400 MHz, $CDCl_3$) δ 8.42 (td, J = 7.9, 1.5 Hz, 1H), 8.35−8.33 (m, 1H), 8.09 (s, 1H), 7.90−7.86 (m, 2H), 7.69 (d, J = 8.2 Hz, 2H), 7.26−7.18 (m, 6H), 6.57−6.51 (m, 4H), 3.74 (s, 3H), 2.39 (s, 3H); ^{13}C NMR (100 MHz, $CDCl_3$) δ 161.9, 158.2, 150.2, 144.8, 143.9, 142.4, 140.7, 140.6, 132.4, 130.1, 130.0, 129.1, 126.3, 125.9, 123.4, 119.4, 119.3, 115.7, 113.9, 105.9, 55.2, 21.4; IR (solid) ν 3061.4, 2838.7, 2217.7, 1569.8, 1479.1, 1417.4, 1316.2, 1254.5, 1133.0, 1087.9 cm^{-1}; HRMS (FAB) m/z calcd for $C_{28}H_{23}N_3O_3S$ [M + H] 482.1538, found 482.1537.

*(Z)-(2-(4-Cyanophenyl)-2-(2-(4-methoxyphenyl)pyridin-1-ium-1-yl)vinyl)(tosyl)amide (**1v**):* purple solid (84.9 mg, 88%); mp 142.2−143.9 °C; ^{1}H NMR (400 MHz, $CDCl_3$) δ 8.52−8.48 (m, 2H), 8.03−8.00 (m, 1H), 7.87 (d, J = 7.7 Hz, 1H), 7.68 (d, J = 8.0 Hz, 2H), 7.58−7.54 (m, 3H), 7.32−7.28 (m, 2H), 7.20 (d, J = 7.9 Hz, 2H), 6.57 (d, J = 8.7 Hz, 2H), 6.41 (d, J = 8.7 Hz, 2H), 3.68 (s, 3H), 2.52 (s, 3H), 2.41 (s, 3H); ^{13}C NMR (100 MHz, $CDCl_3$) δ 196.9, 157.2, 156.5, 150.4, 145.0, 143.4, 140.2, 138.5, 138.1, 135.9, 130.0, 129.0, 128.5, 127.9, 127.3, 125.8, 122.7, 117.4, 114.1, 55.2, 26.6, 21.3; IR (liquid) ν 3059.5, 2996.8, 2836.8, 1685.5, 1509.1, 1483.9, 1337.4, 1250.6, 1132.0, 1082.8 cm^{-1}; HRMS (FAB) m/z calcd for $C_{29}H_{26}N_2O_4S$ [M + H] 499.1692, found 499.1693.

*(Z)-(2-(4-Methoxyphenyl)-2-(2-(4-nitrophenyl)pyridin-1-ium-1-yl)vinyl)(tosyl)amide (**1w**):* purple solid (76.4 mg, 76%); mp 147.1−149.3 °C; ^{1}H NMR (400 MHz, DMSO d_6) δ 8.93 (d, J = 5.4 Hz, 1H), 8.77 (td, J = 7.9, 1.3 Hz, 1H), 8.28−8.22 (m, 2H), 7.73 (d, J = 8.8 Hz, 2H), 7.48−7.45 (m, 5H), 7.23 (d, J = 8.0 Hz, 2H), 6.75−6.68 (m, 4H), 3.67 (s, 3H), 2.38 (s, 3H);^{13}C NMR (100 MHz, DMSO d_6) δ 156.6, 154.4, 150.1, 148.1, 146.3, 144.0, 139.5, 138.1, 137.4, 130.4, 129.5, 129.1, 128.9, 128.5, 125.2, 122.5, 121.9, 115.8, 114.4, 55.0, 20.7; (liquid) ν 3002.6, 2927.4, 2830.0, 1598.7, 1518.7, 1473.4, 1349.9, 1308.5, 1257.4, 1240.9, 1125.3, 1081.9 cm^{-1}; HRMS (FAB) m/z calcd for $C_{27}H_{23}N_3O_5S$ [M + H] 502.1437, found 502.1434.

*3,5-Diphenylimidazo[1,2-a]pyridine (**2a**):* brown solid (46.2 mg, 85%); mp 162.9−164.2 °C; ^{1}H NMR (400 MHz, $CDCl_3$) δ 7.73 (dd, J = 9.0, 1.1 Hz, 1H), 7.65 (s, 1H), 7.30 (dd, J = 9.0, 6.9 Hz, 1H), 7.11−7.04 (m, 3H), 7.03−6.94 (m, 5H), 6.88−6.86 (m, 2H), 6.76 (dd, J = 6.9, 1.1 Hz, 1H); ^{13}C NMR (100 MHz, $CDCl_3$) δ 147.4, 139.0, 134.8, 134.3, 130.8, 128.7, 128.2, 128.2, 127.4, 127.2, 126.8, 126.5, 124.1, 117.0, 115.3; IR (solid) ν 3060.5, 2926.5, 2853.2, 1484.9, 1444.4, 1293.0, 1155.2, 1131.1 cm^{-1}; HRMS (EI) m/z calcd for $C_{19}H_{14}N_2$ [M + H] 270.1157, found 270.1155.

*5-(4-Methoxyphenyl)-3-phenylimidazo[1,2-a]pyridine (**2b**):* brown solid (34.4 mg, 60%); mp 108.4−110.2 °C; ^{1}H NMR (400 MHz, $CDCl_3$) δ 7.59 (d, J = 8.9, 1H), 7.54 (s, 1H), 7.18−7.14 (m, 1H), 6.96−6.92 (m, 1H), 6.89−6.83 (m, 4H), 6.77−6.75 (m, 2H), 6.61 (d, J = 6.8, 1H), 6.40 (d, J = 8.5, 2H), 3.59 (s, 3H); ^{13}C NMR (100 MHz, $CDCl_3$) δ 159.6, 147.5, 138.9, 134.7, 131.0, 129.6, 129.0, 127.2, 126.8, 126.8, 126.4, 124.2, 116.6, 114.9, 112.9, 55.3; IR (solid) ν 3056.6, 3019.0, 2929.3, 2853.2, 1606.4, 1514.8, 1492.6, 1461.8, 1288.2, 1251.6, 1154.2, 1027.9 cm^{-1}; HRMS (EI) m/z calcd for $C_{20}H_{16}N_2O$ [M + H] 300.1263, found 300.1263.

*5-(4-tert-Butylphenyl)-3-phenylimidazo[1,2-a]pyridine (**2c**):* yellow oil (45.4 mg, 70%); ^{1}H NMR (400 MHz, $CDCl_3$) δ 7.72 (dd, J = 9.0, 1.0 Hz, 1H), 7.63 (s, 1H), 7.30−7.26 (m, 1H), 7.00−6.91 (m, 7H), 6.85−6.83 (m, 2H), 6.76 (dd, J = 6.8, 1.0 Hz, 1H), 1.22 (s, 9H); ^{13}C NMR (100 MHz, $CDCl_3$) δ 151.5, 147.4, 139.2, 134.5, 131.2, 131.0, 128.9, 128.0, 127.1, 126.8, 126.4, 124.3, 124.2, 116.7, 114.8, 34.4, 31.1; IR (solid) ν 3059.5, 3030.6, 2961.2, 2927.4, 2866.7, 1603.5, 1537.9, 1519.9, 1495.5, 1479.1, 1460.8, 1394.3, 1362.5, 1295.9, 1157.1 cm^{-1}; HRMS (EI) m/z calcd for $C_{23}H_{22}N_2$ [M + H] 326.1783, found 326.1780.

*3-Phenyl-5-(p-tolyl)-2,3-dihydroimidazo[1,2-a]pyridine (**2d**):* yellow oil (41.8 mg, 74%); ^{1}H NMR (400 MHz, $CDCl_3$) δ 7.64 (dd, J = 9.1, 1.2 Hz, 1H), 7.57 (s, 1H), 7.21 (q, J = 5.4 Hz, 1H), 6.98−6.94 (m, 1H), 6.90−6.84 (m, 4H), 6.80−6.78 (m, 2H), 6.70 (d, J = 7.8 Hz, 2H), 6.67 (d, 6.9 Hz, 1H), 2.14 (s, 3H); ^{13}C NMR (100 MHz, $CDCl_3$) δ 147.5, 139.2, 138.3, 134.6, 131.4, 130.9, 128.9, 128.1, 128.0, 127.1, 126.8, 126.2, 124.1, 116.8, 115.0, 21.1; IR (liquid) ν 3027.7, 2922.6, 2855.1, 1535.1, 1517.7, 1496.5, 1479.1, 1445.4, 1358.6, 1294.9, 1157.1 cm^{-1}; HRMS (EI) m/z calcd for $C_{20}H_{16}N_2$ [M + H] 284.1313, found 284.1312.

*3-Phenyl-5-(m-tolyl)imidazo[1,2-a]pyridine (**2e**):* brown solid (42.2 mg, 79%); mp 155.9−157.3 °C; ^{1}H NMR (400 MHz, $CDCl_3$) δ 7.64 (dd, J = 9.0, 0.9 Hz, 1H), 7.57 (s, 1H), 7.22−7.18 (m, 1H), 6.96−6.88 (m, 5H), 6.82−6.81 (m, 3H), 6.69−6.67 (m, 2H), 1.95 (s, 3H); ^{13}C NMR (100 MHz, $CDCl_3$) δ 147.5, 139.2, 137.0, 134.7, 134.0, 131.1, 129.4, 129.0, 128.5, 127.6, 127.1, 126.8, 126.6, 125.3, 124.1, 116.9, 115.0, 20.9; IR (solid) ν 3076.9, 2935.1, 2854.1, 1508.1, 1477.2, 1446.4, 1295.9, 1155.2 cm^{-1}; HRMS (EI) m/z calcd for $C_{20}H_{16}N_2$ [M + H] 284.1313, found 284.1310.

*5-(4-Fluorophenyl)-3-phenylimidazo[1,2-a]pyridine (**2f**):* brown solid (30.5 mg, 53%); mp 141.0−142.2 °C; ^{1}H NMR (400 MHz, $CDCl_3$) δ 7.67 (d, J = 8.8 Hz, 1H), 7.59(s, 1H), 7.24−7.20 (m, 1H), 7.03−6.94 (m, 5H), 6.82−6.80 (m, 2H), 6.67−6.60 (m, 3H); ^{13}C NMR (100 MHz, $CDCl_3$) δ 163.7, 161.3, 147.4, 137.9, 134.7, 130.7, 130.5, 130.4, 130.2, 130.1, 129.0, 127.4, 126.9, 126.7, 124.1, 117.2, 115.3, 114.6, 114.4; IR (solid) ν 3057.6, 2924.5, 2853.2, 1513.9, 1493.6, 1475.3, 1263.3, 1157.1, 1132.0 cm^{-1}; HRMS (EI) m/z calcd for $C_{19}H_{13}FN_2$ [M + H] 288.1063, found 288.1061.

*5-(4-Chlorophenyl)-3-phenylimidazo[1,2-a]pyridine (**2g**):* brown solid (42.6 mg, 70%); mp 146.9−148.1 °C; ^{1}H NMR (400 MHz, $CDCl_3$) δ 7.74 (dd, J = 8.9, 0.7 Hz, 1H), 7.66 (s, 1H), 7.29 (dd, J = 9.0, 6.9 Hz, 1H), 7.14−7.10 (m, 1H), 7.04−6.95 (m, 6H), 6.88−6.86 (m, 2H), 6.75 (d, J = 6.2 Hz, 1H); ^{13}C NMR (100 MHz, $CDCl_3$) δ 147.4, 137.7, 134.8, 134.4, 132.7, 130.7, 129.5, 129.0, 127.6, 127.4, 126.9, 126.7, 124.0, 117.5, 115.3; IR (solid) ν 3053.7, 2925.5, 2852.2, 1593.9, 1477.2, 1444.4, 1406.8, 1357.6, 1293.0, 1154.2 cm^{-1}; HRMS (EI) m/z calcd for $C_{19}H_{13}ClN_2$ [M + H] 304.0767, found 304.0763.

*1-(4-(3-Phenylimidazo[1,2-a]pyridin-5-yl)phenyl)ethanone (**2h**):* yellow oil (18.2 mg, 29%); ^{1}H NMR (400 MHz, $CDCl_3$) δ 7.71 (dd, J = 9.0, 1.2 Hz, 1H), 7.62 (s, 1H), 7.52−7.50 (m, 2H), 7.28−7.24 (m, 1H), 7.10−7.08 (m, 2H), 6.97−6.87 (m, 3H), 6.82−6.80 (m, 2H), 6.75 (dd, J = 6.9, 1.1 Hz, 1H), 2.44 (s, 3H); ^{13}C NMR (100 MHz, $CDCl_3$) δ 197.2, 147.3, 138.6, 137.6, 136.3, 134.8, 130.6, 128.7, 128.3, 127.4, 127.3, 126.8, 126.6, 124.0, 117.7, 115.7, 26.6; IR (liquid) ν 3029.6, 2923.6, 2853.2, 1683.6, 1514.8, 1494.6, 1445.4, 1358.6, 1295.9, 1156.1 cm^{-1}; HRMS (EI) m/z calcd for $C_{21}H_{16}N_2O$ [M + H] 312.1263, found 312.1262.

*5-(4-Nitrophenyl)-3-phenylimidazo[1,2-a]pyridine (**2i**):* yellow solid (34.8 mg, 52%); mp 177.5−179.7 °C; ^{1}H NMR (400 MHz, $CDCl_3$) δ 7.88−7.84 (m, 2H), 7.81 (d, J = 9.0, 1.1 Hz, 1H), 7.70 (s, 1H), 7.34 (dd, J = 9.0, 6.9 Hz, 1H), 7.25−7.22 (m, 2H), 7.08−7.04 (m, 1H), 7.02−6.98 (m, 2H), 6.90−6.88 (m, 2H), 6.84 (dd, J = 6.9, 1.1 Hz, 1H); ^{13}C NMR (100 MHz, $CDCl_3$) δ 147.2, 147.1, 140.4, 136.3, 135.0, 130.4, 129.0, 128.8, 127.7, 127.4, 126.5, 123.9, 122.6, 118.5, 116.2; IR (liquid) ν 3049.87, 1558.2, 1518.7, 1488.8, 1347.0, 1155.2, 856.2; HRMS (EI) m/z calcd for $C_{19}H_{13}N_3O_2$ [M + H] 315.1008, found 315.1009.

*5-(Naphthalen-2-yl)-3-phenylimidazo[1,2-a]pyridine (**2j**):* brown solid (46.7 mg, 73%); mp 128.1−130.0 °C; ^{1}H NMR (400 MHz, $CDCl_3$) δ 7.70−7.68 (m, 1H), 7.60−7.55 (m, 4H), 7.38−7.33 (m, 2H), 7.30 (d, J = 8.5 Hz, 1H), 7.25 (q, 5.3 Hz, 1H), 6.99−6.96 (m, 1H), 6.81−6.79 (m, 3H), 6.64−6.63 (m, 3H), ^{13}C NMR (100 MHz, $CDCl_3$) δ 147.4, 139.0, 134.7, 132.6, 132.2, 131.8, 130.7, 128.9, 127.9, 127.3, 126.9, 126.5, 126.4, 126.1, 125.5, 124.1, 117.1, 115.5; IR (solid)

DOI: 10.1021/acs.joc.7b00358
J. Org. Chem. 2017, 82, 4352−4361

ν 3052.8, 2923.6, 2853.2, 1502.3, 1479.1, 1443.5, 1288.2, 1154.2 cm^{-1}; HRMS (EI) m/z calcd for $C_{23}H_{16}N_2$ [M + H] 320.1313, found 320.1316.

3-(4-Methoxyphenyl)-5-phenylimidazo[1,2-a]pyridine (**2k**): brown solid (49.1 mg, 82%); mp 95.5−96.3 °C; ^{1}H NMR (400 MHz, $CDCl_3$) δ 7.65 (dd, J = 9.0, 1.2 Hz, 1H), 7.53 (s, 1H), 7.22−7.18 (m, 1H), 7.08−7.03 (m, 1H), 6.99−6.92 (m, 4H), 6.73−6,66 (m, 3H), 6.45−6.41 (m, 2H), 3.65 (s, 3H); ^{13}C NMR (100 MHz, $CDCl_3$) δ 158.4 147.1. 139.0. 134.2. 130.1. 128.4. 128.1. 127.3. 126.5. 123.8. 123.3. 116.9. 115.2. 112.8. 55.2; IR (solid) ν 3058.6, 2924.5, 2852.2, 1508.1, 1482.9, 1445.4, 1294.0, 1243.9, 1154.2, 1028.8 cm^{-1}; HRMS (EI) m/z calcd for $C_{20}H_{16}N_2O$ [M + H] 300.1263, found 300.1260.

3-(4-tert-Butylphenyl)-5-phenylimidazo[1,2-a]pyridine (**2l**): brown solid (49.8 mg, 76%); mp 160.3−161.5 °C; ^{1}H NMR (400 MHz, $CDCl_3$) δ 7.64 (d, J = 8.9 Hz, 1H), 7.56 (s, 1H), 7.21−7.17 (m, 1H), 6.98−6.84 (m, 7H), 6.69 (d, J = 8.2 Hz, 2H), 6.65 (d, J = 6.8 Hz, 1H), 1.15 (s, 9H); ^{13}C NMR (100 MHz, $CDCl_3$) δ 149.6, 147.2, 139.1, 134.2, 128.6, 128.4, 128.0, 127.8, 127.2, 126.8, 124.1, 123.8, 117.0, 115.1, 34.3, 31.1; IR (solid) ν 3055.7, 2956.3, 2862.8, 1531.2, 1482.0, 1448.3, 1292.1, 1264.1, 1151.3, 1019.2 cm^{-1}; HRMS (EI) m/z calcd for $C_{23}H_{22}N_2$ [M + H] 326.1783, found 326.1780.

5-Phenyl-3-(p-tolyl)imidazo[1,2-a]pyridine (**2m**): brown solid (32.4 mg, 65%); mp 144.7−146.3 °C; ^{1}H NMR (400 MHz, $CDCl_3$) δ 7.65 (d, J = 8.9 Hz, 1H), 7.55 (s, 1H), 7.23−7.21 (m, 1H), 7.03−6.90 (m, 5H), 6.68−6.67 (m, 5H), 2.15 (s, 3H); ^{13}C NMR (100 MHz, $CDCl_3$) δ 147.3, 139.0, 136.4, 134.4, 134.3, 129.3, 128.7, 128.3, 128.2, 128.0, 127.3, 126.8, 124.0, 116.9, 115.3, 21.0; IR (solid) ν 3051.8, 2918.7, 2852.2, 1534.1, 1481.1, 1445.4, 1359.6, 1295.9, 1157.1, 1138.8 cm^{-1}; HRMS (EI) m/z calcd for $C_{20}H_{16}N_2$ [M + H] 284.1313, found 284.1315.

3-(4-Bromophenyl)-5-phenylimidazo[1,2-a]pyridine (**2n**): brown solid (40.4 mg, 50%); mp 188.3−189.6 °C; ^{1}H NMR (400 MHz, $CDCl_3$) δ 7.66 (dd, J = 9.0, 1.2 Hz, 1H), 7.56 (s, 1H), 7.26−7.22 (m, 1H), 7.14−7.09 (m, 1H), 7.03−6.97 (m, 6H), 6.71 (dd, J = 6.9, 1.1 Hz, 1H), 6.67−6.64 (m, 2H); ^{13}C NMR (100 MHz, $CDCl_3$) δ 147.6, 138.9, 134.9, 134.2, 130.3, 130.1, 129.8, 128.5, 128.3, 127.7, 125.5, 124.4, 120.8, 117.1, 115.4; IR (solid) ν 3061.4, 2932.2, 2853.2, 1536.0, 1508.1, 1482.0, 1469.5, 1296.9, 1158.0, 1007.6 cm^{-1}; HRMS (EI) m/z calcd for $C_{19}H_{13}BrN_2$ [M + H] 348.0262, found 348.0259.

5-Phenyl-3-(4-(trifluoromethyl)phenyl)imidazo[1,2-a]pyridine (**2o**): brown solid (33.9 mg, 50%); mp 193.5−195.0 °C; ^{1}H NMR (400 MHz, $CDCl_3$) δ 7.78 (dd, J = 9.0, 1.2 Hz, 1H), 7.73 (s, 1H), 7.40−7.36 (m, 1H), 7.23 (d, J = 8.0, 2H), 7.18−7.13 (m, 1H), 7.09−6.99 (m, 6H), 6.84 (dd, J = 6.9, 1.2 Hz, 1H); ^{13}C NMR (100 MHz, $CDCl_3$) δ 147.9, 138.9, 135.2, 134.5, 134.1, 128.9, 128.7, 128.6, 128.2, 128.0, 127.7, 125.3, 124.8, 124.0, 124.0, 124.0, 122.6, 117.2., 115.5; IR (solid) ν 3061.4, 2931.3, 2852.2, 1614.1, 1484.9, 1446.3, 1322.9, 1294.9, 1159.9, 1105.9, 1065.5 cm^{-1}; HRMS (EI) m/z calcd for $C_{20}H_{13}F_3N_2$ [M + H] 338.1031, found 338.1029.

4-(5-Phenylimidazo[1,2-a]pyridin-3-yl)benzonitrile (**2p**): yellow solid (34.5 mg, 45%); mp 212.7−214.5 °C; ^{1}H NMR (400 MHz, $CDCl_3$) δ 7.76 (dd, J = 9.0 Hz, 1.1 Hz, 1H), 7.71 (s, 1H), 7.38 (dd, J = 9.0, 6.9 Hz, 1H), 7.26−7.24 (m, 2H), 7.21−7.16 (m, 1H), 7.10−7.05 (m, 4H), 6.98−6.96 (m, 2H), 6.84 (dd, J = 6.9, 1.1 Hz, 1H); ^{13}C NMR (100 MHz, $CDCl_3$) δ 148.3, 138.8, 135.8, 135.4, 134.2, 130.9, 128.9, 128.5, 128.0, 127.9, 125.2, 124.8, 118.7, 117.2, 115.7, 109.7; IR (liquid) ν 3024.8, 2923.6, 2851.2, 2224.5, 1540.9, 1480.1, 1396.2, 1358.6, 1298.8, 1285.3, 1159.0, 1026.9, 839.8, cm^{-1}; HRMS (EI) m/z calcd for $C_{20}H_{13}N_3$ [M + H]: 295.1109, found295.1107.

3-(4-Nitrophenyl)-5-phenylimidazo[1,2-a]pyridine (**2q**): yellow solid (35.9 mg, 57%); mp 227.3−228.4 °C; ^{1}H NMR (400 MHz, $CDCl_3$) δ 7.85−7.82 (m, 2H), 7.79−7.76 (m, 2H), 7.40 (dd, J = 9.0, 6.9 Hz, 1H), 7.17−7.02 (m, 7H), 6.87 (dd, J = 6.9, 0.9 Hz, 1H); ^{13}C NMR (100 MHz, $CDCl_3$) δ 145.8, 138.9, 137.4, 136.3, 134.4, 129.0, 128.5, 128.1, 128.1, 125.5, 122.4, 117.4, 115.9; IR (liquid) ν 3052.8, 2919.7, 2849.3, 1594.8, 1508.1, 1482.0, 1345.1, 1297.9, 1159.0, 851.4 cm^{-1}; HRMS (EI) m/z calcd for $C_{19}H_{13}N_3O_2$ [M + H] 315.1008, found 315.1010.

3-(3-Methoxyphenyl)-5-phenylimidazo[1,2-a]pyridine (**2r**): brown solid (42.2 mg, 70%); mp 105.8−107.4 °C; ^{1}H NMR (400 MHz, $CDCl_3$) δ 7.65 (dd, J = 9.0, 1.2 Hz, 1H), 7.58 (s, 1H), 7.24−7.19 (m, 1H), 7.07−7.01 (m, 3H), 6.98−6.94 (m, 2H), 6.87−6.83 (m, 1H), 6.70 (dd, J = 6.9, 1.2 Hz, 1H), 6.53−6.48 (m, 2H), 6.27−6.26 (m, 1H), 3.53 (s, 3H); ^{13}C NMR (100 MHz, $CDCl_3$) δ 158.4, 147.4, 139.0, 134.7, 134.4, 132.1, 128.3, 128.3, 128.0, 127.4, 126.5, 124.2, 121.5, 117.0, 115.4, 114.2, 112.9, 54.9; IR (solid) ν 3055.7, 2926.5, 2853.2, 2832.9, 1574.6, 1507.1, 1477.2, 1445.4, 1358.6, 1293.0, 1152.3, 1053.9 cm^{-1}; HRMS (EI) m/z calcd for $C_{20}H_{16}N_2O$ [M + H] 300.1263, found 300.1262.

5-Phenyl-3-(m-tolyl)imidazo[1,2-a]pyridine (**2s**): brown solid (47.4 mg, 84%); mp 104.2−105.2 °C; ^{1}H NMR (400 MHz, $CDCl_3$) δ 7.66−7.64 (m, 1H), 7.57 (s, 1H), 7.22 (dd, J = 8.9, 6.9 Hz, 1H), 7.04−6.92 (m, 5H), 6.87−6.83 (m, 1H), 6.77−6.74 (m, 2H), 6.70−6.68 (m, 1H), 6.48 (s, 1H), 1.98 (s, 3H); ^{13}C NMR (100 MHz, $CDCl_3$) δ 147.4, 139.0, 136.6, 134.5, 134.4, 130.6, 130.0, 128.2, 128.0, 127.4, 127.3, 127.2, 126.9, 125.7, 124.0, 116.9, 115.2, 20.8; IR (solid) ν 3031.6, 2923.6, 2853.2, 1528.4, 1508.1, 1484.8, 1446.4, 1357.6, 1294.0, 1148.4 cm^{-1}; HRMS (EI) m/z calcd for $C_{20}H_{16}N_2$ [M + H] 284.1311, found 284.1309.

3-(3-Fluorophenyl)-5-phenylimidazo[1,2-a]pyridine (**2t**): brown solid (42.0 mg, 73%); mp 118.2−120.8 °C; ^{1}H NMR (400 MHz, $CDCl_3$) δ 7.67 (d, J = 9.1 Hz, 1H), 7.59 (s, 1H), 7.26 (q, J = 5.3 Hz, 1H), 7.09−6.97 (m, 5H), 6.90−6.84 (m, 1H), 6.72 (d, J = 7.0 Hz, 1H), 6.68−6.62 (m, 2H), 6.49−6.46 (m, 1H); ^{13}C NMR (100 MHz, $CDCl_3$) δ 162.9, 160.4, 147.6, 138.9, 135.0, 134.2, 132.9, 132.8, 128.7, 128.6, 128.5, 128.0, 127.6, 125.4, 124.5, 124.5, 124.5, 117.1, 115.8, 115.6, 115.4, 113.6, 113.4; IR (solid) ν 3055.7, 2925.5, 2852.2, 1579.4, 1483.9, 1470.5, 1435.7, 1296.9, 1209.2, 1159.9 cm^{-1}; HRMS (EI) m/z calcd for $C_{19}H_{13}FN_2$ [M + H] 288.1063, found 288.1064.

4-(5-(4-Methoxyphenyl)imidazo[1,2-a]pyridin-3-yl)benzonitrile (**2u**): yellow solid (22.5 mg, 35%); mp 176.9−178.5 °C; ^{1}H NMR (400 MHz, $CDCl_3$) δ 7.74−7.70 (m, 2H), 7.38−7.34 (m, 1H), 7.30−7.28 (m, 2H), 7.00−6.98 (m, 4H), 6.80 (dd, J = 6.9, 1.1 Hz, 1H), 6.59−6.57 (m, 2H), 3.75 (s, 3H); ^{13}C NMR (100 MHz, $CDCl_3$) δ 160.2, 148.3, 138.8, 135.7, 135.6, 130.8, 129.4, 128.8, 126.6, 125.4, 124.8, 118.7, 116.8, 115.4, 113.3, 109.5, 55.4; IR (liquid) ν 3054.7, 2956.3, 2923.6, 2220.6, 1541.8, 1518.7, 1497.5, 1357.6, 1303.6, 1248.7, 1159.9, 1033.7, 836.0 cm^{-1}; HRMS (EI) m/z calcd for $C_{21}H_{15}N_3O$ [M + H] 325.1215, found 325.1212.

1-(4-(3-(4-Methoxyphenyl)imidazo[1,2-a]pyridin-5-yl)phenyl)-ethanone (**2v**): yellow solid (29.0 mg, 42%); mp 136.9−138.4 °C; ^{1}H NMR (400 MHz, $CDCl_3$) δ 7.76 (dd, J = 9.0, 1.0 Hz, 1H), 7.63 (s, 1H), 7.60−7.58 (m, 2H), 7.29 (dd, J = 9.0, 6.9 Hz, 1H), 7.15−7.12 (m, 2H), 6.80−6.77 (m,3H), 6.51−6.48 (m, 2H), 3.67 (s, 3H), 2.52 (s, 3H); ^{13}C NMR (100 MHz, $CDCl_3$) δ 197.3, 158.8, 138.6, 137.7, 136.3, 134.4, 130.2, 128.7, 127.2, 123.7, 123.1, 117.8, 115.5, 113.0, 55.2, 26.5; IR (liquid) ν 2922.6, 2852.2, 1680.7, 1548.6, 1487.8, 1404.9, 1360.5, 1267.0, 1151.3, 1033.7, 962.3 cm^{-1}; HRMS (EI) m/z calcd for $C_{22}H_{18}N_2O_2$ [M + H] 342.1368, found 342.1366.

3-(4-Methoxyphenyl)-5-(4-nitrophenyl)imidazo[1,2-a]pyridine (**2w**): yellow solid (22.0 mg, 32%); mp 191.3−193.8 °C; ^{1}H NMR (400 MHz, $CDCl_3$) δ 7.90−7.86 (m, 2H), 7.81 (dd, J = 9.0, 1.1 Hz, 1H), 7.65 (s, 1H), 7.32 (dd, J = 9.0 6.9 Hz, 1H), 7.24−7.21 (m, 2H), 6.82−6.78 (m, 3H), 6.55−6.52 (m, 2H), 3.68 (s, 3H); ^{13}C NMR (100 MHz, $CDCl_3$) δ 159.2, 147.2, 146.9, 140.4, 136.4, 134.5, 130.3, 129.2, 126.4, 123.7, 122.7, 122.4, 118.5, 116.1, 113.3, 55.3; IR (liquid) ν 2924.5, 2833.9, 1596.8, 1542.8, 1506.1, 1481.1, 1443.5, 1342.2, 1244.8, 1028.8, 836.0 cm^{-1}; HRMS (EI) m/z calcd for $C_{20}H_{15}N_3O_3$ [M + H] 345.1113, found 345.1110.

6-Methyl-3,5-diphenylimidazo[1,2-a]pyridine (**2x**): brown solid (37.2 mg, 65%); mp 151.2−153.4 °C; ^{1}H NMR (400 MHz, $CDCl_3$) δ 7.65 (d, J = 9.0 Hz, 1H), 7.48 (s, 1H), 7.18 (d, J = 9.1 Hz, 1H), 7.07−6.90 (m, 8H), 6.82 (d, J = 7.3, 2H), 2.09 (s, 3H); ^{13}C NMR (100 MHz, $CDCl_3$) δ 146.3, 135.7, 134.7, 132.9, 131.2, 130.0, 129.8, 128.3, 128.1, 127.8, 127.0, 126.4, 120.8, 116.8, 18.5; IR (solid) ν 3060.5, 2924.5, 2853.2, 1483.9, 1475.3, 1443.5, 1289.2, 1244.8, 1159.0 cm^{-1}; HRMS (EI) m/z calcd for $C_{20}H_{16}N_2$ [M + H] 284.1313, found 284.1311.

(Z)-(2-Phenyl-2-(quinolin-1-ium-1-yl)vinyl)(tosyl)amide (**3a**): purple solid (68.1 mg, 85%); mp 205.9−207.4 °C; ^{1}H NMR (400 MHz,

DOI: 10.1021/acs.joc.7b00358
J. Org. Chem. 2017, 82, 4352−4361

DMSO d_6) δ (m, 2H), 8.53 (d, J = 7.1 Hz, 1H), 8.28−8.24 (m, 1H), 8.09 (s, 1H), 8.01−7.94 (m, 3H), 7.41 (d, J = 7.7 Hz, 2H), 7.19−7.17 (m, 4H), 7.03−7.00 (m, 1H), 6.81 (d, J = 7.5 Hz, 2H), 2.32 (s, 3H); ^{13}C NMR (100 MHz, DMSO d_6) δ 153.6, 147.7, 139.3, 135.7, 130.4, 130.2, 129.9, 129.0, 128.7, 125.3, 124.1, 123.0, 119.8, 119.7, 20.8; IR (liquid) ν 3054.7, 2986.2, 1591.9, 1421.3, 1264.1, 1130.1, 1082.8, 964.2 cm^{-1}; HRMS (FAB) m/z calcd for $C_{24}H_{20}N_2S_2O$ [M + H] 401.1324, found 401.1322.

(Z)-(2-(Quinolin-1-ium-1-yl)-2-(p-tolyl)vinyl)(tosyl)amide (**3b**): gray solid (48.3 mg, 58%); mp 165.9−168.1 °C; ^{1}H NMR (400 MHz, $CDCl_3$) δ 8.93 (d, J = 8.2 Hz, 1H), 8.68 (d, J = 5.2 Hz, 1H), 8.20 (s, 1H), 8.09 (d, J = 8.0 Hz, 1H), 8.01 (d, J = 8.7 Hz, 1H), 7.78−7.64 (m, 5H), 7.14 (d, J = 8.0 Hz, 2H), 6.95 (d, J = 8.0 Hz, 2H), 6.63 (d, J = 8.2 Hz, 2H), 2.35 (s, 3H), 2.24 (s, 3H); ^{13}C NMR (100 MHz, $CDCl_3$) δ 152.0, 146.8, 143.3, 140.1, 139.8, 135.2, 134.5, 133.9, 130.4, 130.0, 129.7, 129.6, 128.9, 125.9, 122.0, 120.9, 120.4, 114.6, 21.3, 20.8; IR (liquid) ν 3022.9, 2981.4, 2859.9, 1599.7, 1517.7, 1381.7 cm^{-1}; HRMS (FAB) m/z calcd for $C_{25}H_{22}N_2O_2S$ [M + H] 415.1480, found 415.1478.

(Z)-(2-(4-tert-Butylphenyl)-2-(quinolin-1-ium-1-yl)vinyl)(tosyl)-amide (**3c**): gray solid (47.8 mg, 52%); mp 191.9−192.8 °C; ^{1}H NMR (400 MHz, $CDCl_3$) δ 8.94 (d, J = 8.0 Hz, 1H), 8.68 (d, J = 5.1 Hz, 1H), 8.23 (s, 1H), 8.11 (d, J = 7.6 Hz, 1H), 8.04 (d, J = 8.4 Hz, 1H), 7.79−7.69 (m, 3H), 7.64 (d, J = 7.8 Hz, 2H), 7.17−7.13 (m, 4H), 6.68 (d, J = 8.2 Hz, 2H), 2.36(s, 3H), 1.24(s, 9H); ^{13}C NMR (100 MHz, $CDCl_3$) δ 152.0, 147.8, 146.7, 143.3, 140.3, 140.1, 140.1, 135.4, 133.9, 130.4, 129.9, 129.8, 128.8, 125.9, 125.9, 122.0, 121.1, 120.1, 114.4, 34.3, 31.2, 21.3; IR (solid) ν 3059.5, 2955.4, 1600.6, 1515.8, 1335.5, 1167.7, 1129.1, 1086.7 cm^{-1}; HRMS (FAB) m/z calcd for $C_{28}H_{28}N_2O_2S$ [M + H] 457.1950, found 457.1952.

(Z)-(2-(Quinolin-1-ium-1-yl)-2-(m-tolyl)vinyl)(tosyl)amide (**3d**): purple solid (45.1 mg, 54%); mp 190.1−191.0 °C; ^{1}H NMR (400 MHz, $CDCl_3$) δ 8.92 (d, J = 8.3 Hz, 1H), 8.75 (d, J = 5.6 Hz, 1H), 8.28 (s, 1H), 8.15−8.12 (m, 1H), 8.07−8.04 (m, 1H), 7.84−7.75 (m, 3H), 7.64 (d, J = 8.2 Hz, 2H), 7.14 (d, J = 7.9 Hz, 2H), 7.00 (t, J = 7.7 Hz, 1H), 6.84 (d, J = 7.5 Hz, 1H), 6.74 (s, 1H), 6.37 (d, J = 7.9 Hz, 1H), 2.36 (s, 3H), 2.22 (s, 3H); ^{13}C NMR (100 MHz, $CDCl_3$) δ 152.2, 146.4, 143.3, 140.9, 140.4, 140.1, 138.8, 136.8, 135.4, 130.5, 129.9, 129.8, 128.9, 128.8, 125.9, 125.5, 122.0, 121.2, 121.0, 117.5, 114.3, 21.5, 21.3; IR (liquid) ν 3053.7, 2966.2, 1598.7, 1422.2, 1265.1, 1132.0, 1083.8 cm^{-1}; HRMS (FAB) m/z calcd for $C_{25}H_{22}N_2O_2S$ [M + H] 415.1480, found 415.1479.

1-Phenylimidazo[1,2-a]quinoline (**4a**): white oil (21.3 mg, 42%); ^{1}H NMR (400 MHz, $CDCl_3$) δ 7.78 (dd, J = 7.8, 1.2 Hz, 1H), 7.61−7.50 (m, 9H), 7.39−7.35 (m, 1H), 7.28−7.24 (m, 1H); ^{13}C NMR (100 MHz, $CDCl_3$) δ 145.0, 134.0, 133.4, 131.9, 130.1, 129.1, 128.8, 127.7, 126.4, 124.5, 124.4, 117.6, 116.9; IR (liquid) ν 3050.8, 2923.6, 2854.1, 1442.5, 1380.8, 1292.1, 1126.2 cm^{-1}; HRMS (EI) m/z calcd for $C_{17}H_{12}N_2$ [M + H] 244.1000, found 244.0998.

1-(p-Tolyl)imidazo[1,2-a]quinoline (**4b**): white oil (17.9 mg, 35%); ^{1}H NMR (400 MHz, $CDCl_3$) δ 7.76 (d, J = 7.6 Hz, 1H), 7.60 (t, J = 7.9 Hz, 2H), 7.49 (d, J = 10.9 Hz, 2H), 7.41 (d, J = 7.1 Hz, 2H), 7.37−7.31 (m, 3H), 7.26 (t, J = 7.6 Hz, 1H), 2.48 (s, 3H); ^{13}C NMR (100 MHz, $CDCl_3$) δ 144.9, 138.7, 134.0, 133.3, 130.0, 129.5, 129.0, 128.9, 128.8, 127.6, 126.2, 124.5, 124.4, 117.6, 116.9, 21.4; IR (liquid) ν 3047.0, 2919.7, 2854.1, 1550.5, 1488.8, 1442.5, 1380.8, 1326.8, 1295.9, 1245.8 cm^{-1}; HRMS (EI) m/z calcd for $C_{18}H_{14}N_2$ [M + H]:258.1157, found 258.1154.

1-(4-tert-Butylphenyl)imidazo[1,2-a]quinoline (**4c**): white oil (28.7 mg, 48%); ^{1}H NMR (400 MHz, $CDCl_3$) δ 7.76 (dd, J = 7.8, 1.0 Hz, 1H), 7.63 (d, J = 8.6 Hz, 1H), 7.59 (d, J = 9.4 Hz, 1H), 7.54−7.44 (m, 6H), 7.35 (t, J = 7.2 Hz, 1H), 7.29−7.24 (m, 1H), 1.42 (s, 9H); ^{13}C NMR (100 MHz, $CDCl_3$) δ 151.9, 145.0, 134.1, 133.4, 129.8, 129.0, 128.9, 128.8, 127.6, 126.2, 125.6, 124.5, 124.3, 117.7, 116.9, 34.8, 31.3; IR (liquid) ν 2962.1, 2923.6, 2854.1, 1442.5, 1380.8, 1292.1, 1126.2 cm^{-1}; HRMS (EI) m/z calcd for $C_{21}H_{20}N_2$ [M + H] 300.1626, found 300.1629.

1-(m-Tolyl)imidazo[1,2-a]quinoline (**4d**): white oil (22.6 mg, 45%); ^{1}H NMR (400 MHz, $CDCl_3$) δ 7.77 (dd, J = 7.9, 1.3 Hz, 1H), 7.60−7.58 (m, 2H), 7.51−7.49 (m, 2H), 7.42−7.31 (m, 5H), 7.28−7.24 (m, 1H), 2.43 (s, 3H);^{13}C NMR (100 MHz, $CDCl_3$) δ 145.0, 138.5, 134.0, 133.3, 131.8, 130.7, 129.5, 129.0, 128.9, 128.6, 127.6, 127.2, 126.3, 124.5, 124.4, 117.7, 117.0, 21.4; IR (liquid) ν 3047.0, 2919.7, 2844.1, 1546.6, 1473.4, 1442.5, 1380.8, 1326.8, 1295.9, 1153.2 cm^{-1}; HRMS (EI) m/z calcd for $C_{18}H_{14}N_2$ [M] 258.1157, found 258.1158.

■ ASSOCIATED CONTENT

Supporting Information

The Supporting Information is available free of charge on the ACS Publications website at DOI: 10.1021/acs.joc.7b00358.

NMR spectra, photophysical properties of compounds, and Cartesian coordinates of compounds (PDF)

■ AUTHOR INFORMATION

Corresponding Authors

*E-mail: mbaik2805@kaist.ac.kr.
*E-mail: ejyoo@kangwon.ac.kr.

ORCID

Hong Ki Kim: 0000-0002-6115-384X
Mu-Hyun Baik: 0000-0002-8832-8187

Author Contributions

‖J.Y.L. and J.Y.S. contributed equally to this work.

Notes

The authors declare no competing financial interest.

■ ACKNOWLEDGMENTS

This research was supported by the National Research Foundation of Korea (NRF) (Grant Nos. NRF-2016R1A2B4015351 and NRF- 2016R1A4A1011451), funded by the Korean government. M.-H.B. acknowledges support from the Institute for Basic Science (IBS-R10-D1) in Korea.

■ REFERENCES

(1) (a) *Practical Fluorescence*; Guilbault, G. G., Ed.; Marcel Dekker: New York, 1999. For recent reviews, see: (b) Goncalves, M. S. T. *Chem. Rev.* **2009**, *109*, 190. (c) Kobayashi, H.; Ogawa, M.; Alford, R.; Choyke, P. L.; Urano, Y. *Chem. Rev.* **2010**, *110*, 2620. (d) Li, X.; Gao, X.; Shi, W.; Ma, H. *Chem. Rev.* **2014**, *114*, 590. (e) Tao, Y.; Yuan, K.; Chen, T.; Xu, P.; Li, H.; Chen, R.; Zheng, C.; Zhang, L.; Huang, W. *Adv. Mater.* **2014**, *26*, 7931.

(2) (a) Kim, E.; Koh, M.; Ryu, J.; Park, S. B. *J. Am. Chem. Soc.* **2008**, *130*, 12206. (b) Kim, E.; Koh, M.; Lim, B. J.; Park, S. B. *J. Am. Chem. Soc.* **2011**, *133*, 6642. (c) Namba, K.; Osawa, A.; Ishizaka, S.; Kitamura, N.; Tanino, K. *J. Am. Chem. Soc.* **2011**, *133*, 11466. (d) Namba, K.; Mera, A.; Osawa, A.; Sakuda, E.; Kitamura, N.; Tanino, K. *Org. Lett.* **2012**, *14*, 5554. (e) Liu, B.; Wang, Z.; Wu, N.; Li, M.; You, J.; Lan, J. *Chem.−Eur. J.* **2012**, *18*, 1599. For recent references of color-tunable organic fluorophores, see: (f) Zhao, D.; Hu, J.; Wu, N.; Huang, X.; Qin, X.; Lan, J.; You, J. *Org. Lett.* **2011**, *13*, 6516. (g) Kiprof, P.; Carlson, J. C.; Anderson, D. R.; Nemykin, V. N. *Dalton Trans.* **2013**, *42*, 15120. (h) Cheng, Y.; Li, G.; Liu, Y.; Shi, Y.; Gao, G.; Wu, D.; Lan, J.; You, J. *J. Am. Chem. Soc.* **2016**, *138*, 4730.

(3) (a) Couty, F.; Evano, G. In *Comprehensive Heterocyclic Chemistry III*; Katritzky, A. R., Ramsden, C. A., Scriven, E. F. V., Taylor, R. J. K., Eds.; Elsevier: Oxford, 2008; Vol. *11*, p 409. (b) Gueiffier, A.; Mavel, S.; Lhassani, M.; Elhakmaoui, A.; Snoeck, R.; Andrei, G.; Chavignon, O.; Teulade, J.-C.; Witvrouw, M.; Balzarini, J.; De Clercq, E.; Chapat, J.-P. *J. Med. Chem.* **1998**, *41*, 5108. (c) Rupert, K. C.; Henry, J. R.; Dodd, J. H.; Wadsworth, S. A.; Cavender, D. E.; Olini, G. C.; Fahmy, B.; Siekierka, J. *Bioorg. Med. Chem. Lett.* **2003**, *13*, 347. (d) Hanson, S. M.; Morlock, E. V.; Satyshur, K. A.; Czajkowski, C. *J. Med. Chem.* **2008**, *51*, 7243. (e) Kim, O.; Jeong, Y.; Lee, H.; Hong, S.-S.; Hong, S. *J. Med. Chem.* **2011**, *54*, 2455. (f) Langer, S. Z.; Arbilla, S.; Benavides,

DOI: 10.1021/acs.joc.7b00358
J. Org. Chem. 2017, 82, 4352−4361

J.; Scatton, B. *Adv. Biochem. Psychopharmacol.* **1990**, *46*, 61. (g) Mizushige, K.; Ueda, T.; Yukiiri, K.; Suzuki, H. *Cardiovasc. Drug Rev.* **2002**, *20*, 163. (h) Almirante, L.; Polo, L.; Mugnaini, A.; Provinciali, E.; Rugarli, P.; Biancotti, A.; Gamba, A.; Murmann, W. *J. Med. Chem.* **1965**, *8*, 305.

(4) (a) Burchak, O. N.; Mugherli, L.; Ostuni, M.; Lacapère, J. J.; Balakirev, M. Y. *J. Am. Chem. Soc.* **2011**, *133*, 10058. (b) Li, G.; Gong, W.-T.; Ye, J.-W.; Lin, Y.; Ning, G.-L. *Tetrahedron Lett.* **2011**, *52*, 1313. (c) Khan, A. T.; Basha, R. S.; Lal, M. *Tetrahedron Lett.* **2012**, *53*, 2211. (d) Gong, W.; Gao, P.; Li, G.; Mehdi, H.; Ning, G.; Yu, J. *RSC Adv.* **2014**, *4*, 51268. For references of imidazo[1,2-*a*]pyridines as a ESIPT fluorophores, see: (e) Mutai, T.; Tomoda, H.; Ohkawa, T.; Yabe, Y.; Araki, K. *Angew. Chem. Int. Ed.* **2008**, *47*, 9522. (f) Mutai, T.; Sawatani, H.; Shida, T.; Shono, H.; Araki, K. *J. Org. Chem.* **2013**, *78*, 2482.

(5) For recent reviews of imidazo[1,2-*a*]pyridine synthesis, see: (a) Bagdi, A. K.; Santra, S.; Monir, K.; Hajra, A. *Chem. Commun.* **2015**, *51*, 1555. (b) Pericherla, K.; Kaswan, P.; Pandey, K.; Kumar, A. *Synthesis* **2015**, *47*, 887. (c) Koubachi, J.; El Kazzouli, S.; Bousmina, M.; Guillaumet, G. *Eur. J. Org. Chem.* **2014**, *2014*, 5119.

(6) (a) Hervet, M.; Théry, I.; Gueiffier, A.; Enguehard-Gueiffier, C. *Helv. Chim. Acta* **2003**, *86*, 3461. (b) Kiselyov, A. S. *Tetrahedron Lett.* **2006**, *47*, 2941. (c) Firmansyah, D.; Banasiewicz, M.; Gryko, D. T. *Org. Biomol. Chem.* **2015**, *13*, 1367.

(7) (a) Lee, D. J.; Han, H. S.; Shin, J.; Yoo, E. J. *J. Am. Chem. Soc.* **2014**, *136*, 11606. (b) Lee, D. J.; Ko, D.; Yoo, E. J. *Angew. Chem., Int. Ed.* **2015**, *54*, 13715. (c) Yoo, E. J. *Synlett* **2015**, *26*, 2189.

(8) (a) Douhal, A.; Amat-Guerri, F.; Acuña, A. U. *Angew. Chem., Int. Ed. Engl.* **1997**, *36*, 1514. (b) Shono, H.; Ohkawa, T.; Tomoda, H.; Mutai, T.; Araki, K. *ACS Appl. Mater. Interfaces* **2011**, *3*, 654. (c) Stasyuk, A. J.; Banasiewicz, M.; Cyrański, M. K.; Gryko, D. T. *J. Org. Chem.* **2012**, *77*, 5552. (d) Padalkar, V. S.; Seki, S. *Chem. Soc. Rev.* **2016**, *45*, 169.

(9) (a) Attanasi, O. A.; Davoli, P.; Favi, G.; Filippone, P.; Forni, A.; Moscatelli, G.; Prati, F. *Org. Lett.* **2007**, *9*, 3461. (b) Pintér, Á.; Nyerges, M.; Virányi, A.; Tőke, L. *Tetrahedron Lett.* **2003**, *44*, 2343. (c) Pinho e Melo, T. M. V. D. *Eur. J. Org. Chem.* **2006**, *2006*, 2873. (d) Tóth, J.; Nedves, A.; Dancsó, A.; Blaskó, G.; Tőke, L.; Nyerges, M. *Synthesis* **2007**, *2007*, 1003. (e) Attanasi, O. A.; Caselli, E.; Davoli, P.; Favi, G.; Mantellini, F.; Ori, C.; Prati, F. *Org. Lett.* **2009**, *11*, 2840. (f) Viswambharan, B.; Selvakumar, K.; Madhavan, S.; Shanmugam, P. *Org. Lett.* **2010**, *12*, 2108. (g) Neue, B.; Fröhlich, R.; Würthwein, E.-U. *Z. Naturforsch., B: J. Chem. Sci.* **2012**, *67*, 295. (h) Gong, W.; Gao, P.; Li, G.; Mehdi, H.; Ning, G.; Yu, J. *RSC Adv.* **2014**, *4*, 51268. (i) Novikov, M. S.; Khlebnikov, A. F.; Rostovskii, N. V.; Tcyrulnikov, S.; Suhanova, A. A.; Zavyalov, K. V.; Yufit, D. S. *J. Org. Chem.* **2015**, *80*, 18.

(10) For the reviews of C−H amination, see: (a) Cho, S. H.; Kim, J. Y.; Kwak, J.; Chang, S. *Chem. Soc. Rev.* **2011**, *40*, 5068. (b) Mei, T.-S.; Kou, L.; Ma, S.; Engle, K. M.; Yu, J.-Q. *Synthesis* **2012**, *44*, 1778. (c) Louillat, M.-L.; Patureau, F. W. *Chem. Soc. Rev.* **2014**, *43*, 901. For t selective references of oxidative annulation of *N*-iminopyridinium ylide, see: (d) Mousseau, J. J.; Fortier, A.; Charette, A. B. *Org. Lett.* **2010**, *12*, 516. (e) Mousseau, J. J.; Bull, J. A.; Ladd, C. L.; Fortier, A.; Sustac Roman, D. S.; Charette, A. B. *J. Org. Chem.* **2011**, *76*, 8243. (f) Ding, S.; Yan, Y.; Jiao, N. *Chem. Commun.* **2013**, *49*, 4250. (g) Yang, W.; Chen, J.; Huang, X.; Ding, J.; Liu, M.; Wu, H. *Org. Lett.* **2014**, *16*, 5418.

(11) (a) Yu, X.; Yang, X.; Wu, J. *Org. Biomol. Chem.* **2009**, *7*, 4526. (b) Prasad, B.; Nallapati, S. B.; Kolli, S. K.; Sharma, A. K.; Yellanki, S.; Medisetti, R.; Kulkarni, P.; Sripelly, S.; Mukkanti, K.; Pal, M. *RSC Adv.* **2015**, *5*, 62966.

(12) (a) Iminov, R. T.; Tverdokhlebov, A. V.; Tolmachev, A. A.; Volovenko, Y. M.; Kostyuk, A. N.; Chernega, A. N.; Rusanov, E. B. *Synthesis* **2008**, *2008*, 1535. (b) Rahimizadeh, M.; Pordel, M.; Bakavoli, M.; Eshghi, H. *Dyes Pigm.* **2010**, *86*, 266. (c) Ahmadi, S. J.; Hosseinpour, M.; Sadjadi, S. *Synth. Commun.* **2011**, *41*, 426. (d) Sun, J.; Liu, Z.; Wang, Y.; Xiao, S.; Pei, M.; Zhao, X.; Zhang, G. *RSC Adv.* **2015**, *5*, 100873−100878. (e) Li, Z.; Wu, S.-S.; Luo, Z.-G.; Liu, W.-K.; Feng, C.-T.; Ma, S.-T. *J. Org. Chem.* **2016**, *81*, 4386.

(13) (a) Hammett, L. P. *J. Am. Chem. Soc.* **1937**, *59*, 96. (b) Josey, A. D. Process for the Nucleophilic Substitution of Unactivated Aromatic and Heteroaromatic Substrates US4683091A, 1985. (c) Hansch, C.; Leo, A.; Taft, R. W. *Chem. Rev.* **1991**, *91*, 165.

(14) Ko, C.; Malick, D. K.; Braden, D. A.; Friesner, R. A.; Martinez, T. J. *J. Chem. Phys.* **2008**, *128*, 104103.

(15) Hirata, S.; Head-Gordon, M. *Chem. Phys. Lett.* **1999**, *314*, 291.

(16) Marques, M. A. L.; Gross, E. K. U. *Annu. Rev. Phys. Chem.* **2004**, *55*, 427.

(17) Casida, M. E.; Huix-Rotllant, M. *Annu. Rev. Phys. Chem.* **2012**, *63*, 287.

(18) (a) Lippert, E. *Z. Naturforsch.* **1955**, *10a*, 541−545. (b) Mataga, N.; Kaifu, Y.; Koizumi, M. *Bull. Chem. Soc. Jpn.* **1955**, *28*, 690.

(19) Parr, R. G.; Yang, W. *Density-Functional Theory of Atoms and Molecules*; Oxford University Press: New York, 1989.

(20) Bochevarov, A. D.; Harder, E.; Hughes, T. F.; Greenwood, J. R.; Braden, D. A.; Philipp, D. M.; Rinaldo, D.; Halls, M. D.; Zhang, J.; Friesner, R. A. *Int. J. Quantum Chem.* **2013**, *113*, 2110.

(21) (a) Becke, A. D. *J. Chem. Phys.* **1993**, *98*, 5648. (b) Lee, C. T.; Yang, W.; Parr, R. G. *Phys. Rev. B: Condens. Matter Mater. Phys.* **1988**, *37*, 785.

(22) Ditchfield, R.; Hehre, W. J.; Pople, J. A. *J. Chem. Phys.* **1971**, *54*, 724.

(23) (a) Hay, P. J.; Wadt, W. R. *J. Chem. Phys.* **1985**, *82*, 270. (b) Wadt, W. R.; Hay, P. J. *J. Chem. Phys.* **1985**, *82*, 284. (c) Hay, P. J.; Wadt, W. R. *J. Chem. Phys.* **1985**, *82*, 299.

(24) Dunning, T. H., Jr. *J. Chem. Phys.* **1989**, *90*, 1007.

(25) (a) Marten, B.; Kim, K.; Cortis, C.; Friesner, R. A.; Murphy, R. B.; Ringnalda, M. N.; Sitkoff, D.; Honig, B. *J. Phys. Chem.* **1996**, *100*, 11775. (b) Edinger, S. R.; Cortis, C.; Shenkin, P. S.; Friesner, R. A. *J. Phys. Chem. B* **1997**, *101*, 1190. (c) Friedrichs, M.; Zhou, R.; Edinger, S. R.; Friesner, R. A. *J. Phys. Chem. B* **1999**, *103*, 3057.

(26) Schaftenaar, G.; Noordik, J. H. *J. Comput.-Aided Mol. Des.* **2000**, *14*, 123.

(27) Cortona3D Viewers. http://www.cortona3d.com (accessed Feb 3, 2017).

DOI: 10.1021/acs.joc.7b00358
J. Org. Chem. 2017, 82, 4352−4361